

Tight-binding scheme for impurity states in semiconductors

J. G. Menchero, R. B. Capaz, and Belita Koiller

Instituto de Física, Universidade Federal do Rio de Janeiro, Caixa Postal 68.528, 21945-970 Rio de Janeiro, Brazil

H. Chacham

Departamento de Física, Universidade Federal de Minas Gerais, Caixa Postal 702, 30123-970 Belo Horizonte, MG, Brazil

(Received 27 October 1998)

A tight-binding approach is presented for the calculation of impurity states in semiconductors. The model provides a valid description of acceptors and donors for shallow as well as deep levels, but is expected to be most useful for intermediate levels in which conventional treatments break down. The impurity state is calculated for large supercells containing up to 64 000 atoms, and a finite-size analysis allows extrapolation to the bulk limit. Using this theory, we find very good agreement with experimental results for Ge, Si, and C acceptors in $\text{Al}_x\text{Ga}_{1-x}\text{As}$ alloys. [S0163-1829(99)04804-3]

The usefulness of semiconducting devices depends in large measure on the ability to exploit the electronic properties which result from the introduction of impurities into the host material. Substitutional impurities in which the valence of the core differs by 1 from the valence of the substituted atom constitute a very important class of these systems. For such impurities, the perturbation potential can be divided into two parts: a long-range screened-Coulomb interaction and a short-range potential within the central cell. Roughly speaking, impurities can be classified as either shallow or deep, depending on whether their binding is dominated by the long-range or the short-range potential, respectively. Shallow levels typically occur near the band edges and are spatially extended over thousands of unit cells. Deep levels, on the other hand, typically lie deep within the band gap and are strongly localized in the vicinity of the defect. Both types of impurities are of great importance in determining semiconducting transport properties.

Formally, the problem of shallow impurities was solved as early as the 1950's,^{1,2} with the advent of the so-called effective mass theory (EMT). The EMT rests on several approximations: (i) It is assumed that the perturbation potential is smooth on the atomic scale, so that the discrete lattice may be regarded as a continuum. (ii) It is assumed that the impurity eigenstate can be constructed from Bloch states derived from at most a few energy bands. (iii) It is further assumed that the impurity eigenstate is highly localized in k space, so that only Bloch states near the given k enter the expansion. As a result, in EMT, the entire electronic structure of the host material is characterized by only a few parameters related to the band curvatures near the k point in consideration.

In the case of deep levels, the above assumptions break down. The binding of the impurity by the short-range potential leads to a strong localization in real space, which in turn implies a broad delocalization in k space. Consequently, the impurity state cannot be realistically constructed from Bloch states in the vicinity of a single k point, and therefore the meaning of effective mass is lost. Successful treatments for deep levels typically involve the use of small supercells with an *ab initio* approach.³ However, such methods are computationally expensive and their usefulness is restricted to systems with short-range potentials. As a result, conventional

approaches to deep levels break down for systems in which the impurity wave functions are even moderately delocalized in real space.

Up to now, no computationally feasible approach exists for *intermediate* levels, i.e., impurities for which shallow as well as deep theories break down. In this paper we present a method that provides a valid description for impurities ranging from the shallow to the deep limits.⁴ As a test for the theory, we consider Ge, Si, and C acceptors in $\text{Al}_x\text{Ga}_{1-x}\text{As}$ alloys, whose binding energies have been measured experimentally⁵ for $0 < x < 0.4$. The Ge impurity in particular provides a rigorous testing ground for theory because at $x = 0$ (pure GaAs) the binding energy is relatively shallow (~ 40 meV), but increases rapidly with a strong upward curvature (bowing) to a relatively deep 120 meV by $x = 0.4$.

Our model consists of a single impurity placed in a very large cubic supercell containing $8L^3$ atoms arranged in the zinc-blende structure, where L is the length of the supercell side in units of the conventional lattice parameter. In this work we consider supercells ranging up to $L = 20$ (64 000 atoms), subject to periodic boundary conditions. Generating a crystal by imposing periodicity on the wave function for a supercell containing N primitive cells is equivalent to sampling at N points in the Brillouin zone. Therefore, the large supercells considered in this work correspond to sampling on a very fine mesh in k space.

In order to treat such large systems of atoms and have a good basis for describing the highly-localized deep levels, the electronic structure is calculated within the tight-binding formalism. For the orbital states, we use the sp^3s^* basis set first proposed by Vogl.⁶ We include the spin-orbit interaction in our tight-binding Hamiltonian,^{7,8} which therefore doubles the number basis states to 10 per site. Our Hamiltonian contains terms for the unperturbed lattice as well as for the impurity, and can be written

$$H = \sum_{ij} \sum_{\mu\nu} h_{\mu\nu}^{ij} c_{i\mu}^\dagger c_{j\nu} + \sum_i \sum_{\mu\nu} \lambda_i \langle \mu | l \cdot s | \nu \rangle c_{i\mu}^\dagger c_{i\nu} + \sum_i \sum_{\mu} U(r_i) c_{i\mu}^\dagger c_{i\mu}, \quad (1)$$

where the roman letters denote site indices and the greek letters label the spin orbitals. Here, $h_{\mu\nu}^{ij}$ define the hopping and on-site energies of the electrons and λ_i defines the strength of the spin-orbit interaction on site i . We take the $h_{\mu\nu}^{ij}$ for pure GaAs and AlAs from the recently proposed spin-orbit based parametrization⁸ due to Boykin, and interpolate for $\text{Al}_x\text{Ga}_{1-x}\text{As}$ using the virtual crystal approximation (VCA). In Boykin's parametrization for GaAs, however, the heavy-hole masses are too large, yielding masses of 0.874 along (111) and 0.443 along (100), whereas the experimental values⁹ are 0.750 and 0.340, respectively. Because the binding energy in EMT is proportional to the effective mass, the heavy-hole masses are expected to be particularly important to treat properly. In order to obtain improved agreement with the experimental masses, we scale the GaAs hopping parameters $V_{x,x}$ and $V_{x,y}$ from Ref. 7 by +15%. The resulting heavy-hole masses are 0.734 and 0.375 along (111) and (100), respectively. Such a scaling also leads to an improved agreement with experiment for the light-hole masses along (111) and (100). For AlAs, experimental data is unavailable for the valence-band masses and the theoretical values vary widely,^{10,11} so that no such scaling is performed.

The perturbation potential is given by $U(r_i)$. Away from the impurity, the potential is described by an isotropic q -dependent screening

$$U(r_i) = \frac{e^2}{\epsilon_0 r_i} + A \frac{e^2}{r_i} e^{-\alpha r_i} + (1-A) \frac{e^2}{r_i} e^{-\beta r_i} - \frac{e^2}{\epsilon_0 r_i} e^{-\gamma r_i}, \quad (2)$$

where the screening parameters A , α , β , and γ are taken from Bernholc.¹² For the dielectric constants, we use $\epsilon_0 = 12.56$ for GaAs and $\epsilon_0 = 10.10$ for AlAs. We stress here the long-range nature of the potential, which decays as $1/r$ far from the impurity. Precisely at the impurity site ($r_i = 0$), Eq. (2) is undefined and we take $U(0) \equiv U_0$, where U_0 is a term which contains all central cell effects. We estimated U_0 from *ab initio* calculations by computing the average potential felt by an electron within a sphere of radius R centered about the impurity, with R taken as half the bondlength.¹³ However, this choice of R is somewhat arbitrary, and therefore the *ab initio* results can only serve as a guide. The approach we follow here is to regard U_0 as an adjustable parameter the value of which is chosen to yield the correct binding energy for pure GaAs. Nevertheless, we show below that the values of U_0 used in this work are consistent with the *ab initio* estimates. Once chosen for a given impurity, this value of U_0 is fixed for all x . In this way, any variation in the acceptor binding energy with respect to x is attributed to the electronic response of the host material, and not to central cell effects. This is in accordance with our *ab initio* calculations that show U_0 changes little from GaAs to AlAs.¹³

The acceptor binding energy for a given supercell size is determined as follows: First, the energy E_v at the top of the valence band is calculated for the case of a perfect crystal [i.e., $U(r_i) = 0$ for all i]. This energy is easily found with the aid of Bloch's theorem. The presence of the impurity breaks translational symmetry and introduces states in the gap above E_v . The highest energy \tilde{E}_v of these states yields the ground-state acceptor energy via the simple relation

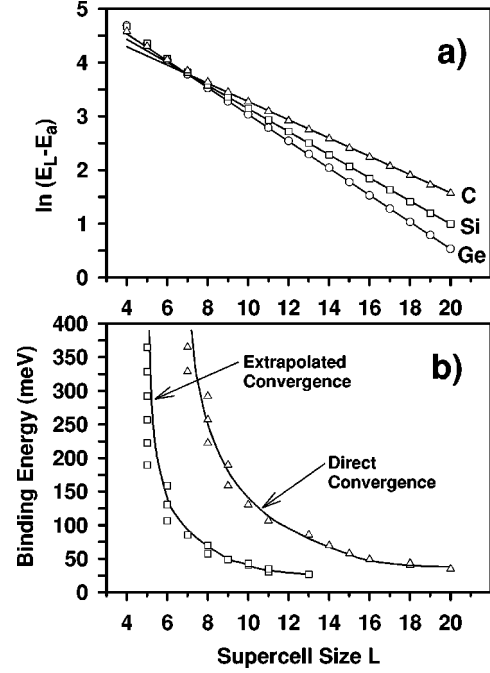


FIG. 1. Finite-size analysis. (a) $\ln(E_L - E_a)$ versus supercell size L for Ge, Si, and C impurities in GaAs. E_L is the acceptor energy (meV) calculated for finite supercells, and E_a is the acceptor energy (meV) in the bulk limit. The excellent fit for $L \geq 8$ indicates the onset of the scaling regime, and corresponds to the size beyond which the wave function is dominated by the exponential tail. (b) Acceptor binding energy in GaAs as a function of the supercell size required to obtain convergence within 3 meV of the bulk limit, both with and without the extrapolation scheme proposed here. The solid lines are guide-to-the-eye fits through the calculated points. Using the extrapolation, the same accuracy can be obtained with far smaller sizes compared to the direct calculation.

$E_a = \tilde{E}_v - E_v$. The primary task therefore is the calculation of this eigenstate. We determine this state by minimizing the expectation value of $\langle \Psi | (H - E_{ref})^2 | \Psi \rangle$, where E_{ref} is a reference energy suitably chosen near \tilde{E}_v .¹⁴ With such an algorithm, the calculation time scales *linearly* with the number of states, making the solution feasible even for extremely large supercells.

In order to investigate extrapolation to the bulk limit, we calculate the acceptor energy for supercell sizes ranging up to $L = 20$ (64 000 atoms). The wave function of a localized bound state is expected to decay with an exponential tail, and we therefore propose a finite-size fit of the form

$$E_L = E_a + \tilde{E} e^{-\alpha L}, \quad (3)$$

where E_L is the acceptor energy for the supercell of size L , and E_a is the acceptor energy in the bulk limit. A plot of $\ln(E_L - E_a)$ versus L should therefore yield a straight line of slope $-\alpha$. In Fig. 1(a) we see that Eq. (3) indeed provides an almost perfect fit to the calculated data for GaAs in the scaling regime $L \geq 8$. In order to determine the acceptor energy in the bulk limit, therefore, it suffices to calculate the acceptor energy E_L for three relatively small supercells of sizes L , $L-1$, and $L-2$, so that the three unknowns in Eq. (3) can be solved. To investigate the practical benefit of such an extrapolation scheme, we have performed the above calcula-

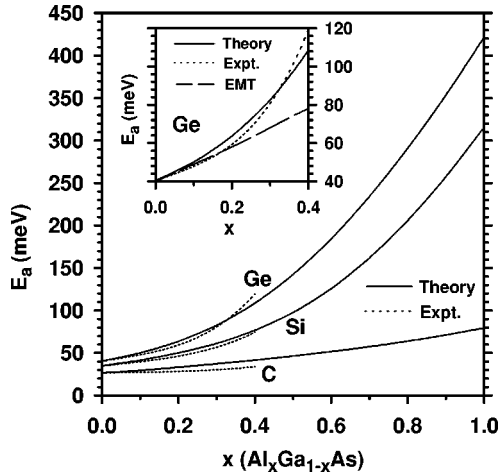


FIG. 2. Calculated acceptor energies E_a for Ge, Si, and C impurities (solid lines) in $\text{Al}_x\text{Ga}_{1-x}\text{As}$. Experimental results are shown for comparison (dashed lines). Inset: Calculated (solid line) and experimental (dashed line) Ge binding energies, together with results calculated using EMT (broken line) (Ref. 10).

tions for acceptors in GaAs with U_0 varying from 0.70 eV to 6.0 eV. This results in acceptor energies ranging from ~ 27 meV up to over 400 meV. We determine the value of L required to obtain convergence within 3 meV of the bulk limit. The calculation is performed in two ways: first using the extrapolation scheme with sizes L , $L-1$, and $L-2$, and second using a single supercell of size L . The results are plotted in Fig. 1(b), and show that the extrapolation scheme in all cases provides the same level of accuracy at far smaller system sizes. Such a finite-size analysis enables us to accurately extrapolate to the bulk limit, even with the use of moderate-size supercells. It is interesting to note that the extrapolated and direct convergence curves seem to saturate at sizes of $L=5$ and $L=7$, respectively. This saturation point is expected to depend on the material in question. For instance, in semiconductors with extremely large effective masses, one would expect the same convergence for smaller sizes.

In Fig. 2 we plot the calculated binding energies (solid lines) for Ge, Si, and C acceptors extrapolated to the $L \rightarrow \infty$ limit. The values of U_0 which yielded the experimental binding energies for pure GaAs were $U_0=2.89$, 2.53, and 0.70 eV for Ge, Si, and C, respectively. These values are consistent in both magnitude and trend with our *ab initio* estimates¹³ of 4.0 eV for Ge and 1.0 eV for C. In Fig. 2 we also plot the experimental binding energies^{5,15,16} (dashed lines) for Ge, Si, and C acceptors in the region $0 < x < 0.4$, obtained in photoluminescence experiments. The calculated results are in very good agreement with experiment for all three impurities, and in particular reproduce the upward “bowing” trend found in going from C to Si to Ge. Interestingly, in all three cases the theoretical curve has a larger slope at $x=0$. A more realistic treatment of the disorder beyond the VCA could possibly account for this discrepancy. Our results indicate that the acceptor binding energy for Ge in AlAs should be ~ 0.42 eV. In the inset of Fig. 2 we reproduce on an enlarged scale the calculated and experimental binding energies for Ge impurities, along with results calculated by Baldereschi, Maschke, and Meloni¹⁰ using EMT (broken line). The EMT results were obtained by scal-

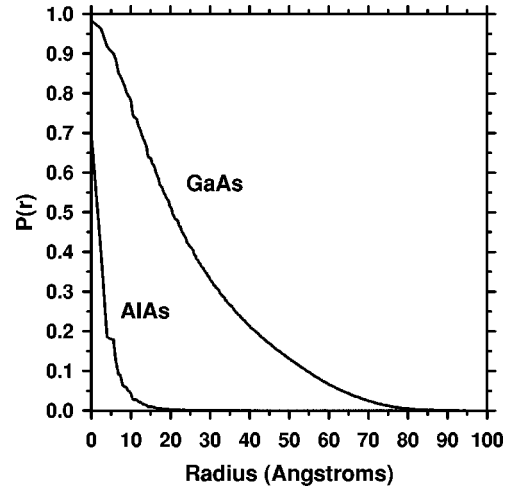


FIG. 3. Probability of finding electron outside a sphere of radius R centered about a Ge impurity in GaAs and AlAs. The value at the origin shows a less than 2% chance of finding the electron on the Ge site for a GaAs host, and more than a 30% chance for an AlAs host.

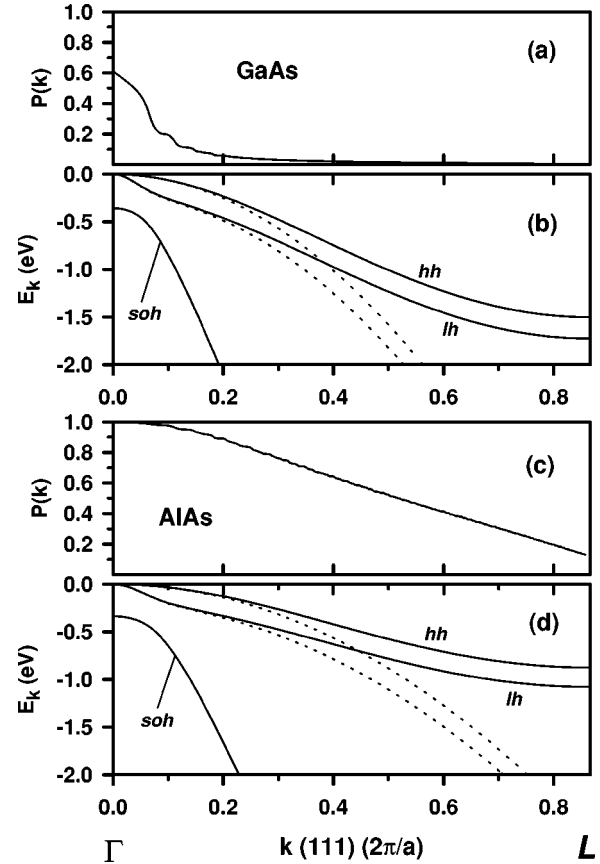


FIG. 4. k -space distribution and valence-band structure for Ge impurities in GaAs and AlAs. (a) Probability of finding electron outside a sphere of radius k for Ge impurities in GaAs. (b) Energy dispersion along (111) for light (lh), heavy (hh), and split-off holes (soh) in GaAs. The $k \cdot p$ dispersion relevant in EMT for the lh and hh is given by the dashed lines. (c) Probability of finding electron outside a sphere of radius k for Ge impurities in AlAs. The probability is broadly distributed over the entire Brillouin zone, indicating a breakdown of the effective mass assumptions. (d) Energy dispersion along (111) for valence band in AlAs, with the $k \cdot p$ dispersion shown for comparison.

ing the $k \cdot p$ matrix elements in order to reproduce the experimental binding energies for GaAs. As can be seen from the inset, the calculated results in this work are in significantly better agreement with experiment than the EMT results. We argue that this is a consequence of the breakdown of the effective mass approximation.

In order to investigate this possibility, we first consider the real-space distribution of the Ge acceptor wave function. In Fig. 3 we plot the probability of finding the electron outside a sphere of radius R centered about the impurity. The value at the origin gives the probability of *not* finding the electron on the Ge site: in other words, there is less than a 2% possibility of finding the electron on the impurity atom in a GaAs host, but more than a 30% chance in an AlAs host. We also see that for Ge in GaAs there is a 60% probability of finding the electron within 25 Å of the Ge atom, whereas for AlAs the 60% probability is obtained already at 2.5 Å. In the tail region, Fig. 3 shows that the impurity wave function in GaAs is essentially completely contained within 80 Å, while for AlAs the containment radius is merely 20 Å. Such a sharp localization for the Ge impurity in AlAs strongly suggests a breakdown of the effective mass approximation.

This breakdown, however, becomes more transparent when viewed from k space. In Fig. 4 we plot for GaAs and AlAs the probability of finding the Ge impurity with wave vector outside a sphere of radius k . We also plot on the same scale the tight-binding energy dispersion (solid lines) from Γ to L for the valence band, together with the $k \cdot p$ dispersion

(dashed lines) calculated within the Luttinger-Kohn model¹⁷ of EMT. Figure 4(a) shows that for GaAs, the wave function is concentrated largely near Γ , in the region where the effective mass approximation is quite good [Fig. 4(b)]. For AlAs, however, the wave function is broadly distributed in k space [Fig. 4(c)], with greater than a 50% probability of finding the electron with $k > \pi/a$. For such large k , Fig. 4(d) shows the large discrepancy which exists between the true dispersion and the $k \cdot p$ dispersion, thereby indicating the breakdown of the effective mass approximation.

In conclusion, we have presented a tight-binding approach for the calculation of impurity states in semiconductors that utilizes an extrapolation scheme to obtain the bulk limit. This method gives good descriptions of shallow as well as deep levels, but is expected to be most useful for intermediate levels in which conventional approaches break down. The method is as simple to apply for donors as for acceptors, and includes spin orbit and mixing with all Bloch states in a natural manner. Although the virtual crystal approximation was employed, the approach can be generalized to include environmental disorder.¹⁸ Finally the extrapolation scheme proposed in this work should prove useful to other (e.g., *ab initio*) supercell methods.

We gratefully acknowledge K. Kamrock and M.V.B. Pinheiro for fruitful discussions. We also thank CNPq, PRONEX, and FINEP for financial support, and NACAD-COPPE/UFRJ for the use of supercomputing facilities.

¹C. Kittel and A. H. Mitchell, Phys. Rev. **96**, 1488 (1954).

²J. M. Luttinger and W. Kohn, Phys. Rev. **97**, 869 (1955).

³See, for instance, C. H. Park and D. J. Chadi, Phys. Rev. Lett. **75**, 1134 (1995); J. Neugebauer and C. G. Van de Walle, *ibid.* **75**, 4452 (1995); T. M. Schmidt, A. Fazzio, and M. J. Caldas, Phys. Rev. B **53**, 1315 (1996).

⁴For deep levels, the impurity is often accompanied by significant lattice relaxations. Such effects are not considered in the present version of this theory.

⁵G. Oelgart, B. Lippold, R. Heilmann, H. Neumann, and B. Jacobs, Phys. Status Solidi A **115**, 257 (1989).

⁶P. Vogl, H. P. Hjalmarson, and J. D. Dow, J. Phys. Chem. Solids **44**, 365 (1983).

⁷D. J. Chadi, Phys. Rev. B **16**, 790 (1977); J. N. Schulman and Yia-Chung Chang, *ibid.* **31**, 2056 (1985).

⁸T. B. Boykin, G. Klimeck, R. C. Bowen, and R. Lake, Phys. Rev. B **56**, 4102 (1997).

⁹B. V. Shanabrook, O. J. Glembocki, D. A. Broido, and W. I. Wang, Phys. Rev. B **39**, 3411 (1989).

¹⁰A. Baldereschi, K. Maschke, and F. Meloni (unpublished).

¹¹*Semiconductors and Semimetals*, edited by R. K. Willardson and

A. C. Beer (Academic, New York, 1975), Vol. 10.

¹²J. Bernholc and S. T. Pantelides, Phys. Rev. B **15**, 4935 (1977).

¹³Our *ab initio* calculations are based on the local-density-functional and pseudopotential approximations with conjugate-gradient minimization of the electronic energy. Cubic supercells with 64 atoms and plane-wave expansions with a cutoff energy of 20 Ry for Ge and 40 Ry for C are used. The central-cell correction is estimated by subtracting the average potential around the impurity from the same quantity around an As atom in the host material.

¹⁴J. K. L. MacDonald, Phys. Rev. **46**, 828 (1934); R. B. Capaz, G. C. de Araujo, Belita Koiller, and J. P. von der Weid, J. Appl. Phys. **74**, 5531 (1993); L. W. Wang and A. Zunger, J. Chem. Phys. **100**, 2394 (1994).

¹⁵G. Oelgart, B. Lippold, M. Proctor, D. Martin, and F. K. Reinhart, Semicond. Sci. Technol. **6**, 1120 (1991).

¹⁶R. Heilmann and G. Oelgart, Semicond. Sci. Technol. **5**, 1040 (1990).

¹⁷R. Enderlein, G. M. Sipahi, L. M. R. Scolfaro, and J. R. Leite, Phys. Status Solidi B **206**, 623 (1998).

¹⁸Belita Koiller and R. B. Capaz, Phys. Rev. Lett. **74**, 769 (1995).